RESEARCH ARTICLE

DESIGN AND APPLICATION OF AC/DC SWITCHING POWER SUPPLY WITH HALF BRIDGE DC/DC CONVERTER TOPOLOGY FOR BATTERY SYSTEMS of ELECTRICAL VEHICLE

Celaletdin AKGÜL[1*], Yücel ÇETİNCEVİZ[2], Erdal ŞEHİRLİ[3]

[1*]Kastamonu University, Faculty of Engineering and Architecture, Electrical and Electronics Engineering, Kastamonu,
eem.celaleddinakgul@gmail.com, ORCID: 0000-0001-7214-9478
[2]Kastamonu University, Faculty of Engineering and Architecture, Electrical and Electronics Engineering, Kastamonu,
ycetinceviz@kastamonu.edu.tr, ORCID: 0000-0001-6834-9442
[3]Kastamonu University, Faculty of Engineering and Architecture, Electrical and Electronics Engineering, Kastamonu,
esehirli@kastamonu.edu.tr, ORCID: 0000-0003-0822-3201

ABSTRACT

This study presents design, analysis and application details of electrical vehicle battery charge device based on half bridge DC-DC converter. Half bridge DC-DC converter in the paper has 620 W power, 25 kHz switching frequency and input DC voltage is obtained by uncontrolled bridge rectifier. In addition, information about the battery that is charged, and battery pack are given. Besides, a protection structure of battery is added by measuring both current and voltage of battery. Firstly, equations required for half bridge DC-DC converter is derived and simulation of battery charge circuit is realized by using PSIM and MATLAB/Simulink. Then, the results of the experimental study and the simulation results are given comparatively. The experimental results prove the accuracy of the simulation studies.

Keywords: *Half Bridge DC-DC Converter, Electrical Vehicle, Battery, MATLAB/Simulink, Application.*

1. INTRODUCTION

Nowadays, interest to the alternative and renewable energy sources has been increasing much because of decreasing fossil sources and fossil sources has negative factors such as climate change, increasing of carbon dioxide rate, decrease of oxygen, air pollution, global warming, negative effect to human health. Recently, the use and the tendency of using of renewable energy sources has increased much. Besides, due to the negative effect of the fossil sources, electrical vehicle has becoming more popular and in future it is assumed that the electrical vehicle will take place of fossil fuel-based vehicles. In addition, electrical vehicle consists of some key components including battery, battery charger, electrical motor, and motor driver. However, the most important part is battery and battery charger of

149

the electrical vehicle. To charge battery of electrical vehicle, DC power source is required. This DC source is provided by switching power supply [1, 2, 3].

As a battery type for electrical vehicle the best option for today is lead-acid, nickel-cadmium, nickel-metal, lithium-ion, and zinc-air [4, 5, 6]. Especially, lithium-ion batteries because of having higher power density are the most preferable battery type [7, 8, 9]. Operation and operation safety of lithium-ion batteries are so important for the use in electrical vehicle [10]. Also, lithium-ion batteries have higher reliability, higher power density, long lasting, lower discharge rate, and higher efficiency features [11]. To obtain higher power value with desired voltage levels, each battery cells are connected series and parallel [12]. On the other hand, the most important problem in electrical vehicle is the limitation of the battery such as weight, cost, limited charge capacity, short driving distance, long charge duration [13]. So, fast charging specification having different kind of DC-DC converter topology ensure the use of electrical vehicle for continuous driving [14].

Efficiency is so important topic for switching power supply. Higher efficiency can be obtained by optimum design of magnetic materials, lower switching losses at the switch on and off conditions. In addition, switching power supply can operate with higher switching frequency rate from kHz to MHz, higher switching frequency provides reducing the size of equipment used in the converter [15]. Also, switching power supply ensures wide input voltage range, lower loss, higher efficiency, weight, and size comparing to linear power supplies.

It is hard to choose switching power supply topologies for low or medium power level. For lower and medium power levels, push-pull and half bridge converter are more popular than full bridge converter [16]. For 200 W – 1000 W power level, generally half bridge topology is preferred, also in half bridge topology, a capacitor is added to primary winding [17]. The biggest disadvantage of push-pull converter is voltage stress which is twice of input voltage [17,18]. However, the main advantage of the half bridge converter regarding to push-pull converter is the construction of primary windings. In push pull converter, the primary should be wounded by two equally windings that causes design difficulty. In addition, half of dc source voltage is applied to the primary windings of half bridge converter but in push pull converter total dc source voltage is applied to half of primary windings. It is also mentioned in literature that the push-pull converter is more suitable for low voltage applications, and it has higher voltage stress on power switches. Nevertheless, push-pull converter has an easiness of driving power switches because it has two low side power switches which can be driving without the need of isolation or bootstrap driving principle. Advantage of half bridge converter comparing to push-pull converter is not having middle point of primary winding that provides easiness for applications [16]. In addition, comparing of full bridge converter, voltage stress of the half bridge converter is nearly half due to the splitted capacitor connection to the primary of transformer. Therefore, half bridge converter is preferable than push-pull and full bridge converters.

For power converter, to conduct their simulations there are a few software such as PSIM and MATLAB providing simulation capability of the converters with higher accuracy [19,20,21,22].

In this paper, by using half bridge DC-DC converter, for electrical vehicle design, simulation and application of batter charge device is realized. Modeling, control design and evaluation of the performance of charger device is conducted by PSIM and MATLAB/Simulink software. Half bridge

DC-DC converter-based battery charger is designed for 620 W power with 112 V output voltage. Design details are also given in this paper and measurements are conducted to validate the applications. In addition, battery back construction is included in the paper. Besides, a protection structure of battery is added by measuring both current and voltage of battery.

2. HALF BRIDGE DC-DC CONVERTER

Single phase AC is converter to DC by diode bridge circuit. Resulting DC is applied to the half bridge DC-DC converter. Half bridge DC-DC converter consists of two power switches, capacitors at input and output, high frequency transformer, high frequency rectifier circuit, and an inductor. After, applying DC, to the power switches, because the power switches are switched on one by one, a high frequency AC on the transformer is obtained. Resulting high frequency AC, is converter to DC by using high frequency diode rectifier. To avoid short circuits because of switch on and off condition of Q_1 and Q_2, dead time is adjusted. During the dead time, energy for load is supplied by inductor L.

As shown in Fig. 1, there are four operation mode of the half bridge DC-DC converter.
1.   Operation mode 1, Q_1 is switched on, Q_2 is switched off.
2.   Operation mode 2, Q_1 and Q_2 are switched off.
3.   Operation more 3, Q_1 is switched off, Q_2 is switched on.
4.   Operation mode 2, Q_1 and Q_2 are switched off.

Square wave AC voltage is occurred at primary windings after the operation of the Q_1 and Q_2 of half bridge DC-DC converter. The square waveform voltage at secondary of the transformer can be obtained lower or higher than primary winding voltage. AC square wave voltage at secondary winding is rectified by D_1 and D_2 diodes. After filtering of the secondary voltage, output voltage V_o is obtained. At Fig. 2., steady state wave forms of half bridge DC-DC converter are shown.

At mode 1, Q_1 is switched on, Q_2 is switched off, D_1 is switched on, D_2 is switched off. Primary winding of the high frequency transformer is connected to mid-point of the series connected capacitors. So, primary winding voltage is equal to $V_{dc}/2$.

When the Q_1 switch is on, there is a voltage drop on the primary winding resulting induced voltage on secondary winding. The induced secondary voltage is rectified by diode and after LC filtering transferred to R load. Secondary voltage can be calculated by (1).

$$V_{se} = \frac{N_s}{N_p}\left(\frac{V_{dc}}{2}\right) \qquad\qquad \#(1)$$

Voltage at output inductor is calculated by (2).

$$V_{L1} = \frac{N_s}{N_p}\left(\frac{V_{dc}}{2}\right) - V_O \qquad\qquad \#(2)$$

Current change of the inductor i_{L1} is equal to (3).

$$\frac{di_{L1}}{dt} = \frac{v_{L1}}{L1} = \frac{1}{L1}\left[\frac{N_s}{N_p}\left(\frac{V_{dc}}{2}\right) - V_O\right] \qquad \#(3)$$

Peak inductor current i_{L1} (pk) can be found at $t=kT$ by (4) [24].

$$I_{L1(pk)} = I_{L1}(0) + \frac{1}{L1}\left[\frac{N_{s1}}{N_p}\left(\frac{V_{dc}}{2}\right) - V_O\right]kT \qquad \#(4)$$

At mode 2, Q_1 and Q_2 switches are off. So, $kT < t <= T/2$ is valid. Diodes at secondary side are forced for conduction by magnetizing current. Decreasing rate of $\dot{I}_{L1}$ can be found by (5) [24].

$$\frac{di_{L1}}{dt} = -\frac{V_o}{L_1} \qquad 0 < t \leq (0.5 - k)T \qquad \#(5)$$

Initial value of i_{L1} can be calculated by (6).

$$I_{L1}(0) = i_{L1}[t = (0.5 - k)T] = I_{L1(pk)} - \frac{V_O(0.5 - k)T}{L_1} \qquad \#(6)$$

At mode 3, Q_1 is switched off, Q_2 is switched on, D_2 is switched on, D_1 is switched on. The voltage on primary winding is equal to $-V_{dc}/2$. Reverse operation of mode 1 is realized. V_o output voltage can be found by the integral in (7) [24].

$$V_O = 2 * \left[\int_0^{kT}\left(\frac{N_{s1}}{N_p}\left(\frac{V_{dc}}{2}\right) - V_O\right)dt + \int_k^{T/2} -V_O dt\right] \qquad \#(7)$$

Output voltage can be calculated by (8).

$$V_O = \frac{N_{s1}}{N_p}V_{dc}k \qquad \#(8)$$

Output power is calculated by (9).

$$P_O = V_O I_L = \eta P_i = \eta\frac{V_{dc}I_{p(avg)}k}{2} \qquad \#(9)$$

$I_{p(avg)}$ average primary current can be calculated by (10).
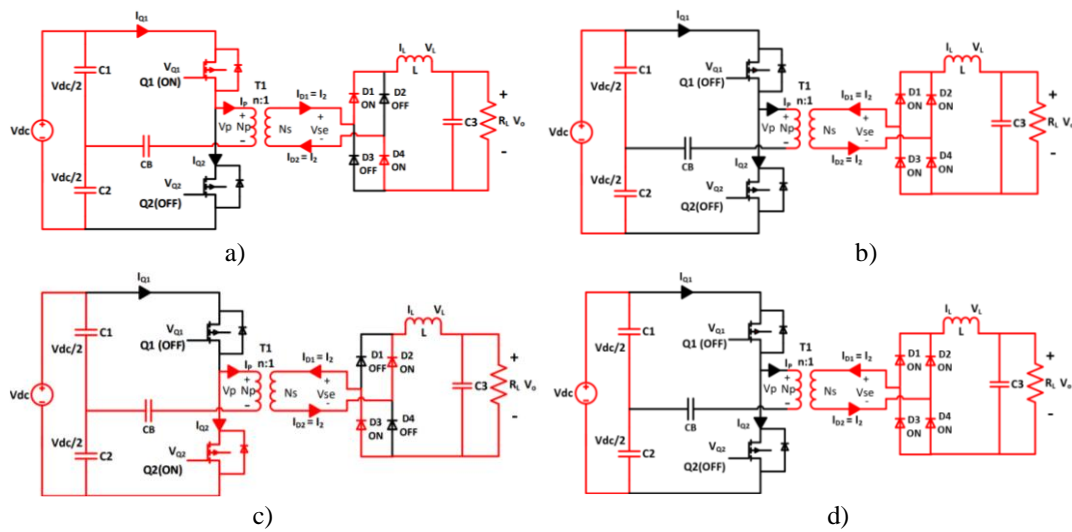
$$I_{p(avg)} = \frac{2P_o}{\eta V_{dc} k_{max}}$$ #(10)

Drain current of Q_1 and Q_2 is found by (11).

$$I_{d(max)} = I_{p(avg)} = \frac{2P_O}{\eta V_{dc} k_{max}}$$ #(11)

Maximum voltage on switch is equals to (12).

$$V_{c(max)} = V_{dc(max)}$$ #(12)

Maximum duty cycle k cannot be more than 50%. Half bridge DC-DC converter is generally used for medium power applications with the 350 W- 800 W power range [24].


Figure 1. Operation modes of half bridge DC-DC converter, Mode 1, Q_1 is on Q_2 is off (a), Mode 2 (b), Q_1 and Q_2 is off, Mode 3 (c), Q_1 is off Q_2 is on, Mode 4, Q_1 and Q_2 is off (d).

In every operation mode, the VQ1 + VQ2= Vdc equation which is derived by Kirchoff voltage Law of closed loop regarding Vdc and both Q1 and Q2 switches voltages, should be verified. So, by neglecting the switch on state voltage drops, at Mode 1 0 + VQ2= Vdc, at Mode 2 VQ1 + VQ2= Vdc, at Mode 3 VQ1 + 0 = Vdc, at Mode 4 VQ1 + VQ2= Vdc.
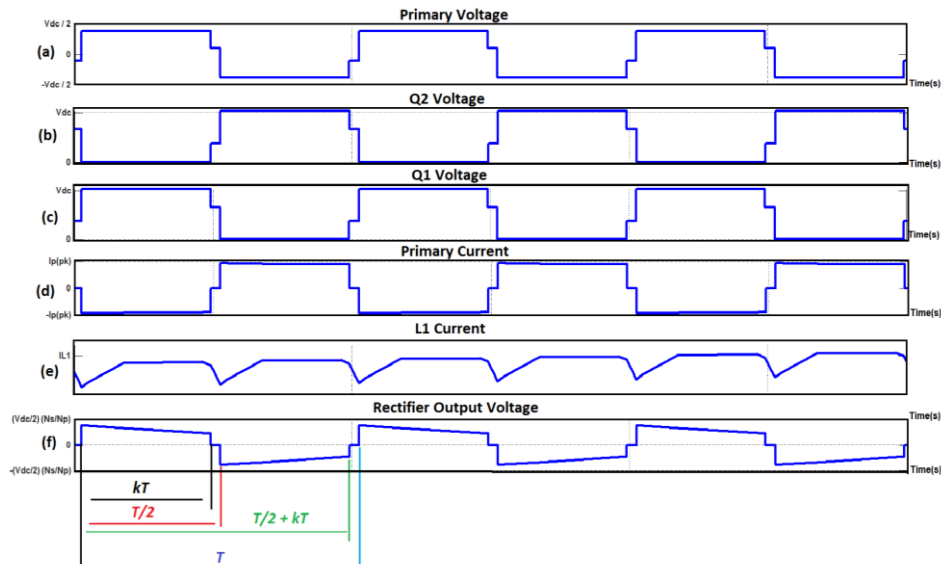
Figure 2. Steady-state wave form of half bridge converter at continuous conduction mode. Primary voltage (a), Q_2 voltage (b), Q_1 voltage (c), primary current (d), L_1 current (e), rectifier output voltage (f).

3. DESING OF HALF BRIDGE DC-DC CONVERTER
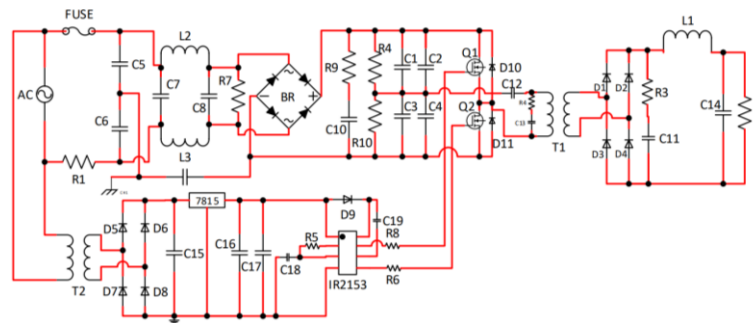
Figure 3. Half bridge DC-DC converter application circuit.

Application circuit of half bridge DC-DC converter is shown in Fig.3. In this circuit, IR2153 MOSFET driver integrated circuit is used. AC grid voltage is converter to DC voltage by diode bridge. Capacitors parallels to each other is charged by half of DC voltage. High frequency transformer is connected between the midpoint of capacitors and power switches. To reduce the high frequency noise due to the power switches, filter is added between AC grid and diode bridge. In addition, for protection of power switches, parallel RC snubber circuit and diodes are used. For

powering of IR2153 IC with 15 V, second transformer and diode bridge are used. Applied converter parameters are defined as 25 kHz switching frequency, 750 W output power and 0.8 efficiency. In addition, for transformer, ETD 54 core with N87 material of EPCOS company is chosen. Besides, for output inductor, ETD39 core with N87 material of EPCOS company is used. Also, litz wire is employed both transformer and inductor.

3.1. Design of High Frequency Transformer
Require calculations for transformer is achieved by using (13-18).

$$V_{inmax} = V_{rms} * \sqrt{2} \tag{#(13)}$$

$$P = V * I, \quad P_{out} = 700W, \quad V_{out} = 110V \implies I_{out} = 6,36A \tag{#(14)}$$

$$P_{in} = {P_{out}}/{\eta}, \quad I_{in} = {P_{out}}/{311} = 2,81A \tag{#(15)}$$

Dead time is set as 1 µs. Total period is 40 µs because the switching frequency is 25 kHz. Voltage is occurred in primary 49% of total period, when it is thought that 2 µs dead time each two-half period. Duty cycle and conduction time is as in (16).

$$D = {(100 - 2)}/{2} = \%49, t_{on} = \%49 * 40\mu s = 19.6\mu s \tag{#(16)}$$

Primary turn number N_p can be calculated in (17) when magnetic flux density (B) is taken as 100 mT. A_e is cross sectional area of the core.

$$N_p = {V_{in} * t_{on}}/{2 * \Delta B * A_e} \tag{#(17)}$$

Secondary turn number can be calculated by (18).

$$N_s = {N_p * V_{out}}/{2 * D * V_{in}} \tag{#(18)}$$

Required conductor number of litz wire and cross-sectional area of the conductor can be calculated by (19-23). I_p primary current, S cross sectional area, J current density.

$$S = {I_p}/{J} \tag{#(19)}$$

When the frequency of the current passing through the conductor is increased, current passes surface of h conductor. It is called as skin effect. In (20), skin depth that is the depth of the current passing from conductor while frequency change is given. In the application, operating frequency is 35 kHz, so skin depth is calculated as 0.45 mm.

$$\delta = {72}/{\sqrt{f}} \qquad\qquad \#(20)$$

Transformer and inductor are wound by conductor having 0.3 mm diameter. For primary and secondary windings, parallel conductor number is calculated by using (19), (21), (22).

$$S = \pi r^2 \qquad\qquad \#(21)$$

$$S = {I_s}/{J} \qquad\qquad \#(22)$$

For output side inductor, required calculations are done by using (24). ΔI inductor ripple current, is taken as 20% of output current.

$$L_{out} = {(V_{in} - V_{out}) * D * T}/{2 * \Delta I} \qquad\qquad \#(24)$$

In application, as a power switch IXTQ460P2 power MOSFET, as a parallel diode of MOSFET, MUR460, as rectifier diodes DSEP15-06A are used.
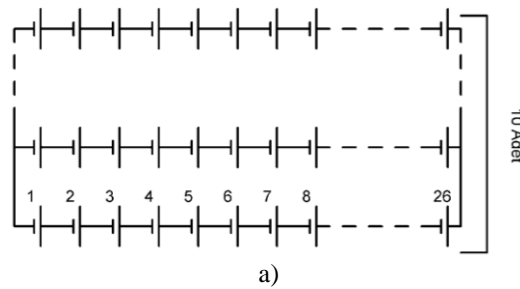
3.2. Battery Pack
Battery pack is obtained series and parallel combination of li-ion battery cell having 3,6 V value. Total parallel battery cell number is 10 and total series connected battery cell number is 26. Parameter of battery pack is given in Table 1.

Table 1. Battery pack parameters.

Parameter	Value
Battery Cell Capacity	3450 mAh
Battery Nominal Voltage	3,6 V
Parallel connection number	10
Battery capacity	34,5 Ah
Series connection number	26
Maximum Voltage	109,2 V

Each battery cell capacity is 3450 mAh and nominal voltage is 3.6 V. Battery pack structure and battery pack is shown in Fig. 4. As it is seen, there are 10 parallel connection and 26 series connection of each battery cell.


a)

b)

Figure 4. Battery pack connection circuit (a), battery pack (b).

3.3. Simulation Results

Before the applications of half bridge DC-DC converter-based battery charger, at first, simulation studies are conducted. To conduct simulations, Matlab/Simulink and PSIM software are used. Firstly, simulation study is realized by resistor as a load then battery in Matlab/Simulink. After that, for validation of the Matlab/Simulink, PSIM simulation is made via resistor as a load.

Firstly, simulation is conducted by using resistors as a load and its Matlab/Simulink circuit is given in Fig. 5. Protection circuit by measuring current and voltage of the battery is seen by the figure. Via protection logic, at the condition of higher current and voltage more than defined limit the converter stops its operation. Besides, required dead time between the operation of the switch is added in the simulations as it is seen by the figure.
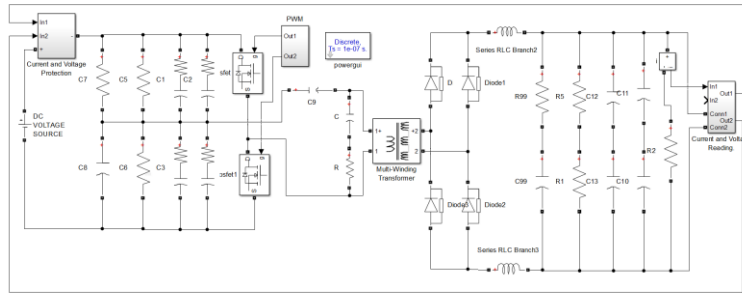
Figure 5. Matlab/Simulink simulation circuit resistor as a load.

In Fig. 6 switching signals of the switches are seen. Dead time between each switch can be observed easily by the figure and it is set as 1 μs. After applying the signal in Fig. 6 to the switches, operation of the converter is realized.
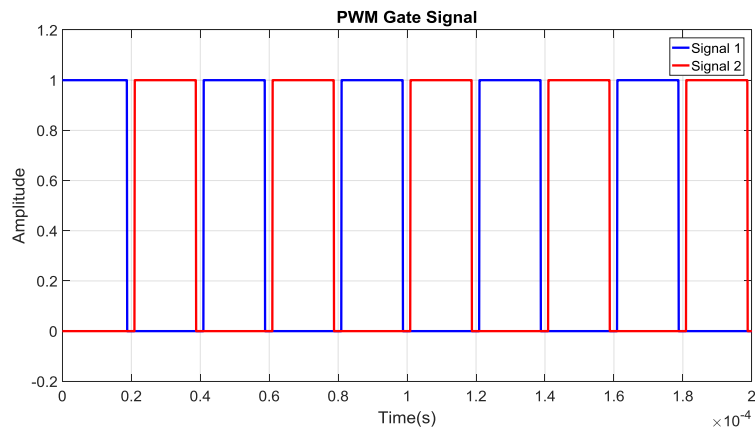

Figure 6. Switching signals of power switches.

After applying the signals in Fig. 6 to the power switches, high frequency AC voltage is induced at the secondary windings of the transformer as given in Fig. 7. Zero voltage values in the figure are because of the dead time between each switch.
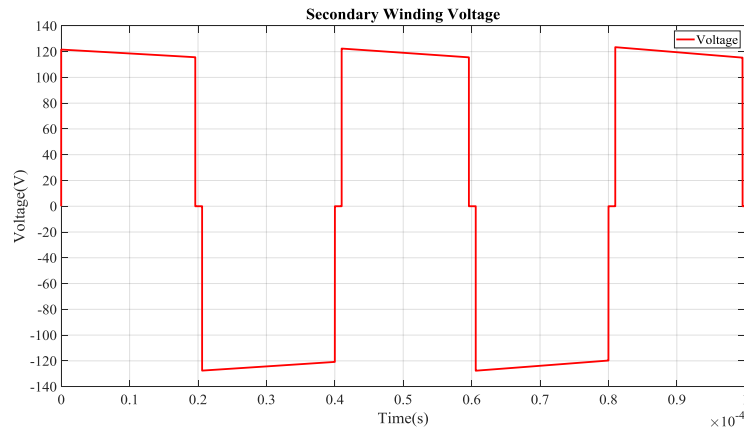
Figure 7. Voltage waveform of transformer secondary winding.

Switching signals in Fig. 6 results in drain-source voltages of power switches given in Fig. 8, after applying the power to the converter. It is seen that the drain-source voltage does not include peak values which is an advantage of the topology.
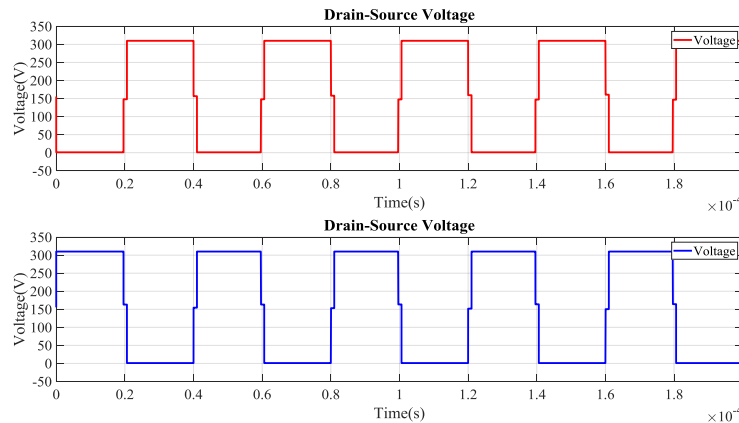
Figure 8. Drain source voltage of MOSFET 1 and MOSFET2.

After operation of each power switches, primary winding of the transformer has a voltage drop as given in Fig. 9. Also transferring energy to the secondary windings causes current drawn by primary winding that is given in Fig. 9. Because of the dead time between switches, both current and voltage has zero values.
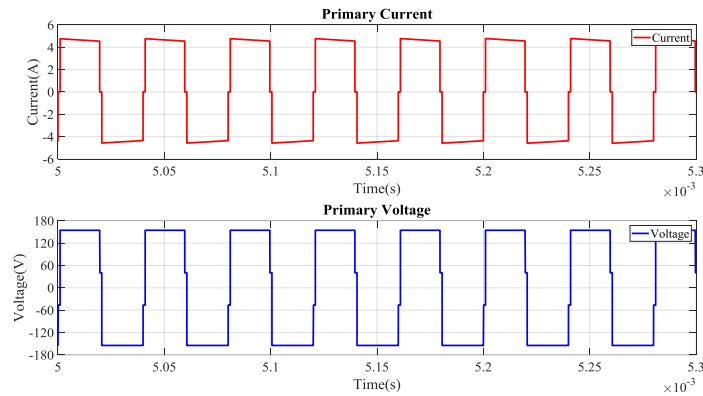
Figure 9. Transformer primary winding voltage and current.

After inducing voltage at secondary, high frequency AC voltage is rectified by the high frequency diode bridge and applied to the load via inductor. Therefore, resulting load voltage and current are given in Fig. 10. The load voltage is obtained as 113.6 V and load current is obtained as 5.6 A.
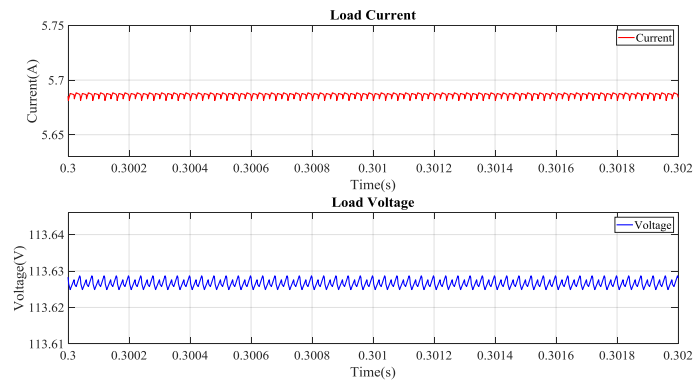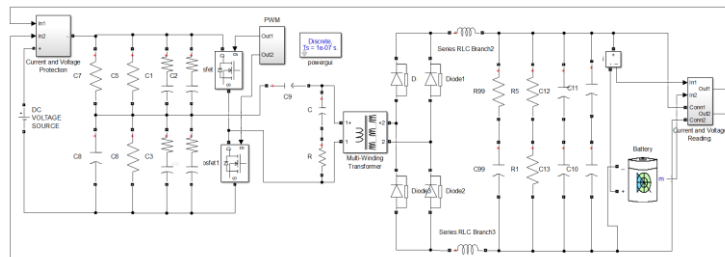

Figure 10. Load voltage and current.

Fig. 11. A graph of the V and I power waveforms of the MOSFET is shown.

(a)   (b)
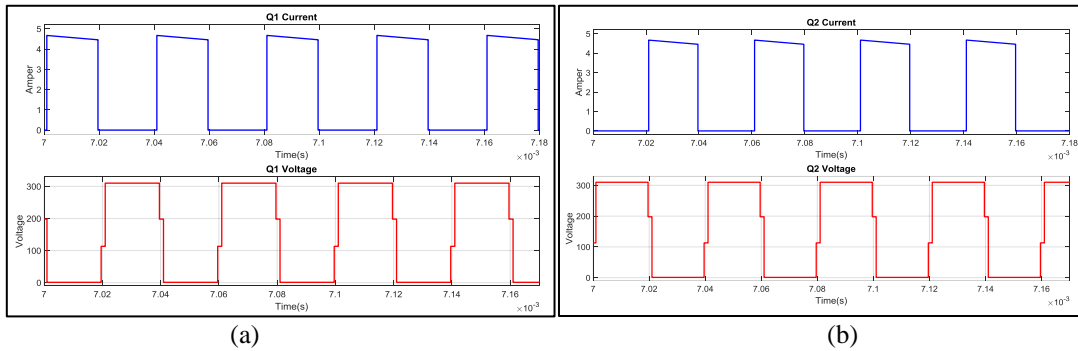
Figure 11. V and I waveforms of the MOSFET. (a) Q1 V and I waveforms, (b) Q2 V and I waveforms.

Simulation study in Matlab/Simulink is also carried out by using Li/Ion battery as a load and the simulation circuit is given in Fig. 12.
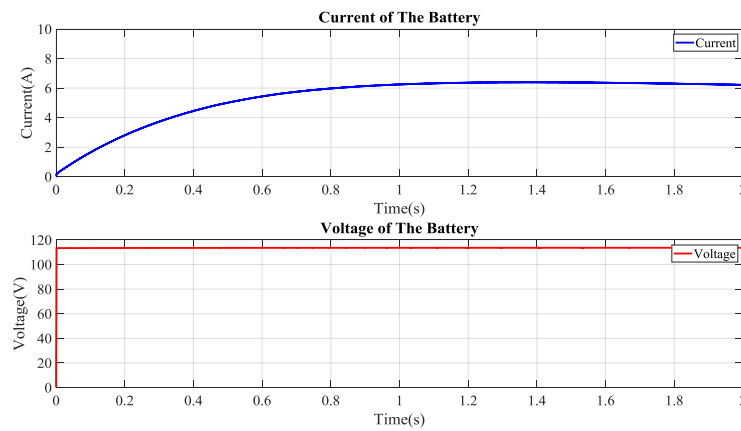

Figure 12. Matlab/Simulink simulation circuit Li/Ion battery as a load.

After the operation of the converter, the battery is charged. To observe the charging situation of the battery, SOC value is observed as given in Fig. 13. It is depicted that the SOC is increasing meaning that the batter is charging.

161
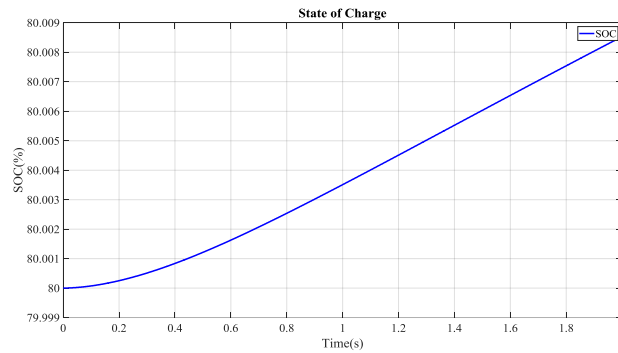
Figure 13. Li/Ion battery state of charge (SOC).

In order to provide charging of Li/Ion battery, there should be enough output voltage as given in Fig 14. In addition, while the charging process with the SOC in Fig 13., the battery draws current from the converter as shown in Fig. 14.

Figure 14. Li/Ion battery voltage and current.

To validate the results conducted with Matlab/Simulink, simulation study is conducted with PSIM software. The simulation circuit of PSIM is given in Fig. 15.
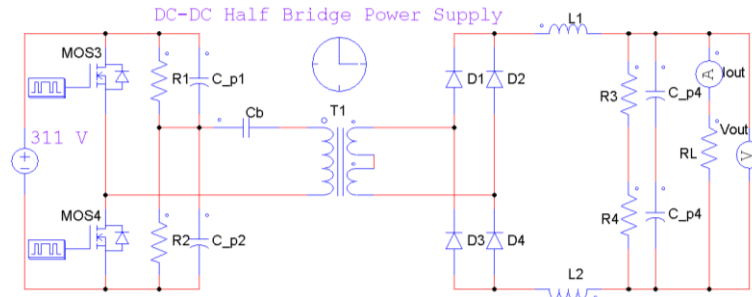
Figure 15. PSIM simulation circuit.

After operation of the converter with a resistor as load in PSIM, the output voltage and current are obtained as given in Fig. 16. It is observed by the simulation the output voltage is 110 V and output current is 6.2 A.
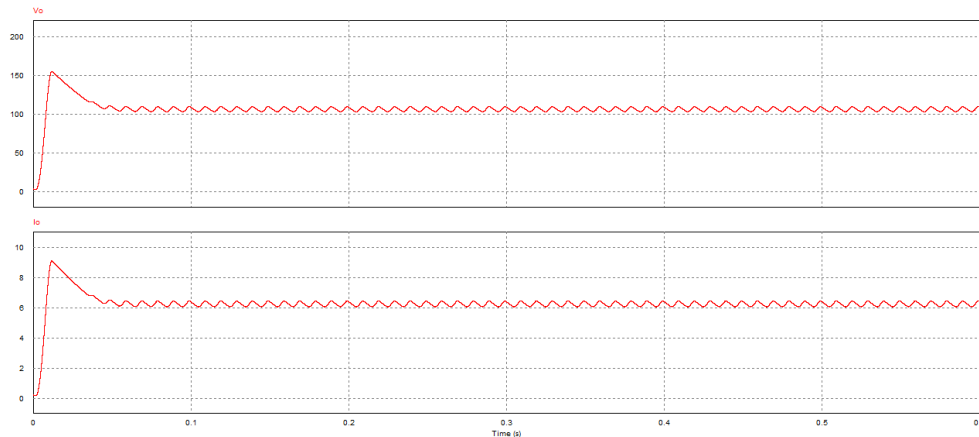
Figure 16. Output voltage and current of the PSIM simulation.

3.4. Material Selection

On the base of simulation studies, application of half bridge DC-DC converter is realized. For the converter, materials used in the application is selected as given in Table .2.

Table 2. Half bridge dc-dc converter material list.

Material	Part Number	Material Values	Size(mm)
C1 and C2	KENDEIL K054006810PM0E050	400V and 680µF -40°C-+105°C	(D x L) 35.00 x 50.00

163

C_B	FARATRONİC C42P2105KBSC400	275VAC and 1μF -40°C-+125°C	(W x H x T) 32.0 x 18.00 x 9.00
D1 and D2	IXYS DSEP15-06A	600V and 15A -55°C-+150°C	TO220AC PACKAGE
Q1 and Q2	IXYS IXTQ460P2	500V and 24A -55°C-+150°C	TO3P PACKAGE

4. EXPERIMENT

Circuit parameters of half bridge DC-DC converter for application are defined as follows.
V_{in} = 311V
V_{out} = 112V
I_o = 5.5A
fs = 25 kHz
η = (P_{out} / P_{in}) * 100 = (620.48/697.5) * 100 = % 88.9
In addition, material values for half bridge DC-DC converter are given below.
Magnetic core= ETD54/28/19
Material = N87 EPCOS
Q1 – Q2: IXTQ460P2 - MOSFET DIS.24A 500V, $R_{DS (on)} \leq 270m\Omega$,
Diode: DSEP15-06A (15A 600V) -TO-220AC

Circuit connection diagram of the half bridge DC-DC converter-based battery charger is given in Fig. 17. Charging of the battery takes much time, therefore experiments are conducted by using resistive load and measurements are taken by using resistive load. However, the converter is tested with battery as well. The converter control is realized with open loop structure through IR2153 IC. Furthermore, the IC has dead time generator internally and dead time is set as 1 μs Besides, protection circuit is added with Arduino microcontroller by measuring current and voltage. As a current sensor ACS712 type sensor is used. Voltage is measured with voltage divider.
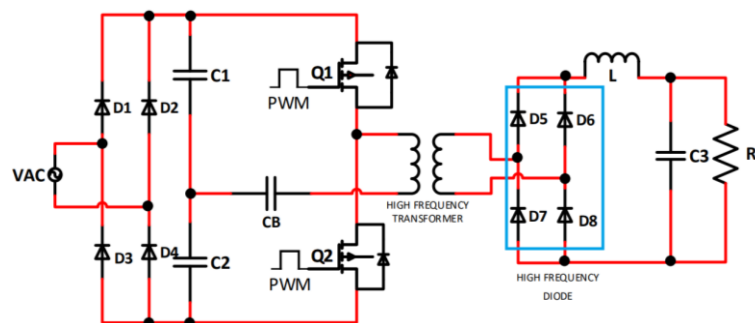
Figure 17. Half bridge DC-DC converter-based charger connections.

The battery charger is installed in the electrical vehicle as shown in Fig. 18, also protection circuit is given in the same figure. The battery pack is connected to the electrical motor of the vehicle in the figure.
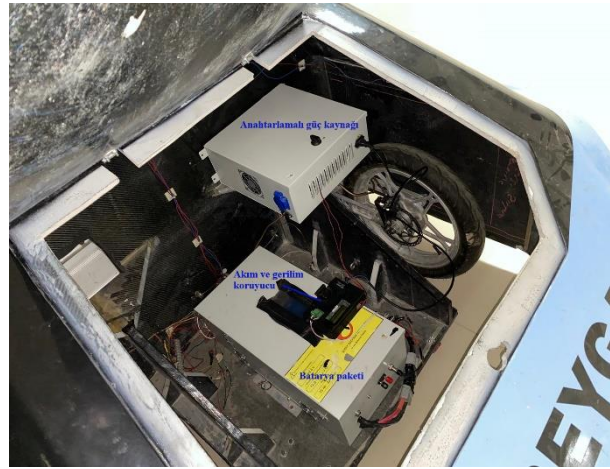
Figure 18. Installation of the battery charger to the electrical vehicle.

Fig. 19 shows the half bridge DC-DC converter-based battery charger circuit feeding resistive load and measurement units. Also, for protection of the battery and the charger, a protection circuit measuring battery current and voltage using Arduino Nano micro controller is done. In addition, an LCD screen is used to visualize battery voltage and current. Fig 19 also shows the measurement results that output voltage and current values of the load with multimeters as 5.54 A output current and 112 V output voltage.

**Figure 19.** Application setup and measurements.

Fig. 20 shows the output current of the load by oscilloscope. Output current is measured by ACS 712 current sensor and oscilloscope probe is connected to ACS 712 output to measure the output current

waveform. When it is calculated by the oscilloscope measurement results regarding to ACS712 output voltage, output current is approximately obtained as 5.54 A. Instead of using current probe, which is expensive, such way of current measurements is more practical and cheaper. However, in Fig. 20, ACS712 provides analog output as a voltage, this seems confusing. But after calculations regarding to ACS 712 output voltage, output current is found as approximately 5.54 A.
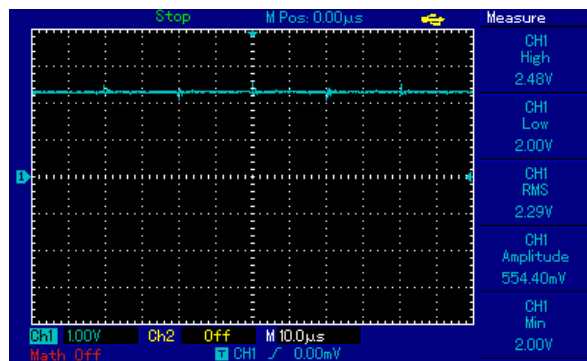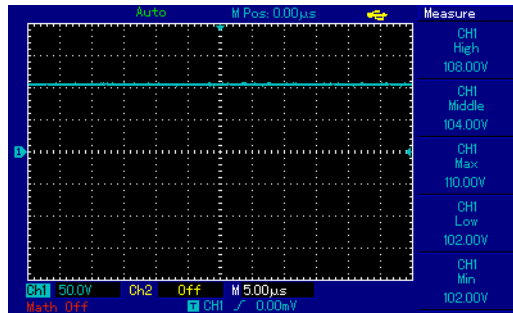

Figure 20. Load current as an output voltage of the ACS 712 current sensor.
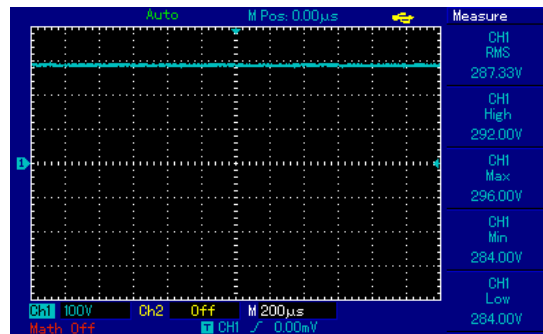
The waveform of the input, output and rectified input voltage of the converter is given in Figure 21. The input voltage is 146 V, the output voltage is 110V and the rectified input voltage is measured as 296 V.
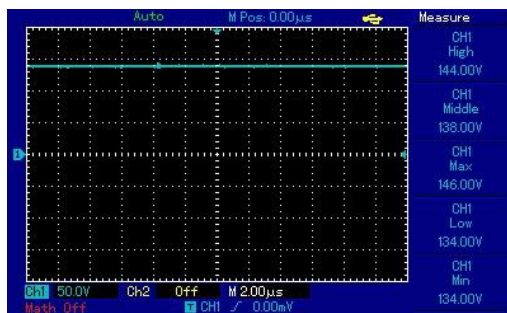
(a)   (b)

(c)

Figure 21. Voltage results of half bridge dc to dc converter. (a) Input voltage, (b) Output voltage, (c) Rectified input voltage.

Gate-source PWM signals of Q_1-Q_2 power switches having 1 μs dead time is given in Fig. 22. Similar to the simulation results in Fig. 7, application has also the same waveform.
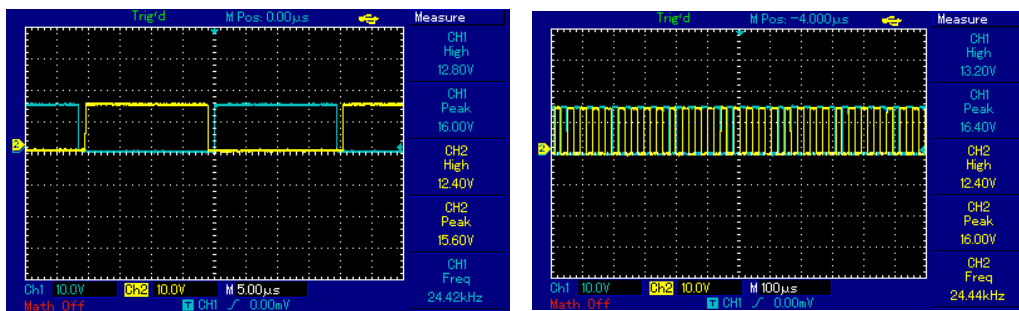
(a)   (b)

Figure 22. Switching signals of power switches, a) 5 μs time scale, b) 100 μs time scale.

After applying signals given in Fig 22, the voltage on primary winding is obtained as high frequency square wave and given in Fig. 23. IT is seen that there is no peak value on primary voltage, it is the same waveform as by the simulation results in Fig. 10. So, simulation results prove the application.

Figure 23. Primary voltage waveform of the converter.

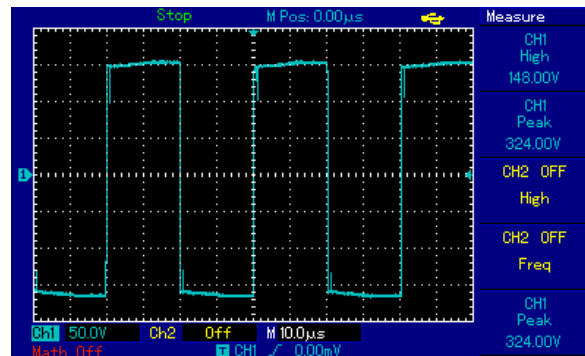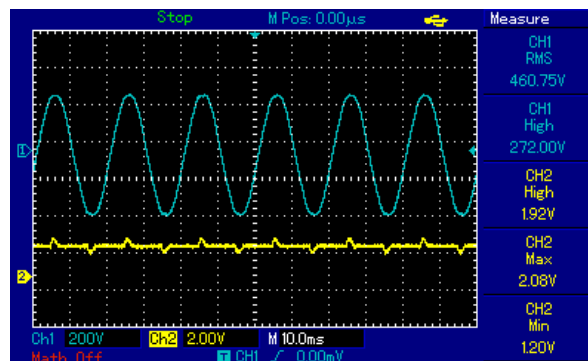Half bridge DC/DC converter is connected to the sinusoidal grid by diode bridge. The grid voltage and current is shown in Fig 24. It is seen that sinusoidal voltage is obtained, as 220 V. But the grid current is not sinusoidal because of the higher valued capacitor at the DC side.

Figure 24. AC voltage and current of the converter under load.

5. DISCUSSION

Design, simulation, and application of battery charge device for electrical vehicle by using half bridge DC-DC converter topology for up to 620 W and its protection system including current and voltage protection is presented in the study. The half bridge DC-DC topology is one of the power converter topologies providing moderate or higher power conversion. By changing turns ratio of high frequency transformer, it ensures lower or higher output DC voltage. In addition, as an advantage of the topology, the converter has two power switches and lower voltage stress on the switches. So, the converter is very convenient as a battery charging device. Therefore, both application and simulations prove assumed results successfully that is charging the Li/Ion battery while ensuring protection. For the simulation, MATLAB/Simulink and PSIM software are used. Simulation results including protection structure approve the applications. [25] presents half bridge DC-DC converter focusing on

power factor correction for battery charging of the electrical vehicle but the protection of the battery is not covered as it presented in the paper. Although, full-bridge and DAB based electrical vehicle battery charger are presented in [26], [27] for higher power, number of switch and voltage stress on the power switches are higher than presented study. [28] presents electrical vehicle charger based on LLC converter, but it does not present battery package structure as it is given presented study and have higher number of power switches increasing cost. However, presented study includes just DC-DC conversion, power factor correction is not a scope of the study. To have higher power factor, another front-end converter is good to be added to have higher power factor as future work.

6. CONCLUSION

In this study, design, simulation, and application of battery charge device for electrical vehicle by using half bridge DC-DC converter topology is presented. Modeling of charge device its control scheme design and evaluation of its performance is conducted by MATLAB/Simulink and PSIM environment. Besides, battery pack consisting of 260 single battery cells used for charging is presented. In experimental study, current and voltage graphs of half bridge DC-DC converter at 620 W full load with 25 kHz switching frequency are obtained and it is observed that the charge device presents desired performance. Besides, protection of the battery pack is provided by using both current and voltage measurements. If the battery draws more than allowable current limit and battery voltage drop is more than maximum voltage, the battery charger stops its operation as a protection which is so important for increasing battery lifetime. Application results of charging and protection are also validated by simulation studies.

Closed loop application by using microcontroller and linear control techniques after modeling the converter is aimed to be conducted as a future study. In order to realize closed loop application, an isolated voltage measurement circuit will also be designed.

ACKNOWLEDGEMENT

REFERENCES

[1] Collin, A. J., Djokic, S. Z., Thomas, H. F., and Meyer, J. (2011, October). Modelling of electric vehicle chargers for power system analysis. In *11th International Conference on Electrical Power Quality and Utilisation* (pp. 1-6). IEEE.

[2] Safayatullah, M. D., Elrais, M. T., Ghosh, S. andRezaii, R. (2022). A comprehensive review of power converter topologies and control methods for electric vehicle fast charging applications. *IEEE Access*, 10, 40754-40793.

[3] Khalid, M., Ahmad, F., Panigrahi, B. J., and Al-fagih, L. (2022) A comprehensive review on advanced charging topologies and methodologies for electric vehicle battery. *Journal of Energy Storage*, 53, 105084.

[4] Oman, H. (1998, November). On-board energy and power management on electric vehicles: effect of battery type. In *17th DASC. AIAA/IEEE/SAE. Digital Avionics Systems Conference. Proceedings (Cat. No. 98CH36267)* (Vol. 2, pp. I43-1). IEEE.

[5] Martins, L. S., Guimares, L. F., Junior, A. B. B., Tenorio, J. A. S., and Espinoza, D. C. R. (2021) Electric car battery: An overview on global demand, recycling and future approaches towards sustainability. *Journal of Environmental Management*, 295(1), 113091.

[6] Liaqat, M., Ghadi, Y. Y., Adnan, M. and Fazal, M. R. (2022). Multicriteria Evaluation of Portable Energy Storage Technologies for Electric Vehicles. *IEEE Access*, 10, 64890-64903.

[7] Kim, T. H., Park, J. S., Chang, S. K., Choi, S., Ryu, J. H., and Song, H. K. (2012). The current move of lithium-ion batteries towards the next phase. *Advanced Energy Materials*, 2(7), 860-872.

[8] Elmahallawy, M., Elfouly, T., Alouani, A. and Massoud, A. M. (2022). A Comprehensive Review of Lithium-IonBatteries Modeling, and State of Health and Remaining Useful Lifetime Prediction. *IEEE Access*, 10, 119040-119070.

[9] Chen, W., Liang, J., Yang, Z., and Li, G. (2021) A Review of Lithium-Ion Battery for Electric Vehicle Applications and Beyond. *Energy Procedia*, 158, 4363-4368.

[10] Duan, J., Tang, X., Dai, H., Yang, Y., Wu, W., Wei, X., and Huang, Y. (2020). Building safe lithium-ion batteries for electric vehicles: a review. *Electrochemical Energy Reviews*, 3(1), 1-42.

[11] Umair Ali, M., Hussain Nengroo, S., Adil Khan, M., Zeb, K., Ahmad Kamran, M., and Kim, H. J. (2018). A real-time simulink interfaced fast-charging methodology of lithium-ion batteries under temperature feedback with fuzzy logic control. *Energies*, 11(5), 1122.

[12] Kılıç, E. (2019). Da-da yükselten dönüştürücü ile elektrikli araç batarya şarj cihazi tasarimi. *Kahramanmaraş Sütçü İmam Üniversitesi Mühendislik Bilimleri Dergisi*, 22(4), 281-287.

[13] Chéron, E., and Zins, M. (1997). Electric vehicle purchasing intentions: The concern over battery charge duration. *Transportation Research Part A: Policy and Practice*, 31(3), 235-243.

[14] LaMonaca, S., and Ryan, L. (2022). The state of play in electric vehicle charging services−A review of infrastructure provision, players, and policies. *Renewable and Sustainable Energy Reviews*, 154, 111733.

[15] Majid, A. (2012). Analysis and implementation of switch mode power supplies in MHz frequency region (Doctoral dissertation, Mid Sweden University).

[16] Hung, Y. C., Shyu, F. S., Lin, C. J., and Lai, Y. S. (2003, November). New voltage balance technique for capacitors of symmetrical half-bridge converter with current mode control. In The Fifth International Conference on Power Electronics and Drive Systems, 2003. PEDS 2003. (Vol. 1, pp. 365-369). IEEE.

[17] Al-Badrani, H., Ameen, Y. M., and Kadir, M. N. A. (2021, October). An AC/DC switch mode power supply based on half bridge DC/DC converter for low power applications. In *2021 12th International Renewable Energy Congress (IREC)* (pp. 1-6). IEEE.

[18] Hung, Y. C., Shyu, F. S., Lin, C. J., and Lai, Y. S. (2003, November). Design and implementation of symmetrical half-bridge DC-DC converter. In *The Fifth International Conference on Power Electronics and Drive Systems, 2003. PEDS 2003.* (Vol. 1, pp. 338-342). IEEE.

[19] Randall Shafer, "Fundamentals of Power Electronics with Matlab", Charles River Media, 1st ed., 2007.

[20] Armata J.M, Besrest B., Pauly R.,"PSIM/MATLAB cosimulation for electrical architectures global models", AES 2005

[21] Khader, S., Hadad, A., and Abu-Aisheh, A. A. (2011, April). The application of psim and matlab/simulink in power electronics courses. In 2011 IEEE Global Engineering Education Conference (EDUCON) (pp. 118-121). IEEE.

[22] Mehar, H. (2013). The case study of simulation of power converter circuits using Psim software in teaching. *American Journal of Educational Research*, *1*(4), 137-142.

[23] Asadi, F., and Eguchi, K. (2021). Power Electronics Circuit Analysis with PSIM®. In *Power Electronics Circuit Analysis with PSIM®.* De Gruyter.

[24] Muhammad, R. H., Narendra, K., and Ashish, R. K. (2014). Power Electronics Devices, Circuits and Applications. *Pearson Education*.

[25] Kushwaha, R., and Singh, B. (2022) A Bridgeless Isolated Half-Bridge Converter Based EV Charger With Power Factor Preregulation. *IEEE Transactions on Industry Applications* 58(3), 3967-3976.

[26] Park, Y., Chakraborty, S. and Khaligh, A. (2022) DAB Converter for EV Onboard Chargers Using Bare-Die SiC MOSFETs and Leakage-Integrated Planar Transformer. *IEEE Transactions on Transportation Electrification* 8(1), 209-224.

[27] Mendoza-Varela, I. A., Alvarez-Diazcomas, A., Rodriguez-Resendiz, J., and Martinez-Prado, M. A. (2021) Modeling and Control of a Phase-Shifted Full-Bridge Converter for a LiFePO4 Battery Charger. *MDPI Electronics* 10(21), 2568.

[28] Al-Attar, H., Hamida, M. A., Ghanes, M., and Taleb, M. (2022) LLC DC-DC Converter Performances Improvement for Bidirectional Electric Vehicle Charger Application. *MDPI World Electric Vehicle Journal* 13(1), 2.

NOMENCLATURE

f_s	Switching frequency
P_{out}	Output power
V_{out}	Output voltage
I_{out}	Output current
P_{in}	Input power
I_{in}	Input Current
t_{on}	Conduction Time
A_e	Magnetic core window field
B	Magnetic flux density
S	Cross sectional area
J	Current density
□	Skin depth
L_{out}	Output coil inductance
V_{dc}	Input voltage
V_o	Output voltage
$V_{c(max)}$	Maximum voltage on switch
$V_{in(max)}$	Maximum input voltage
V_{rms}	Stands for root-mean-square voltage
V_{L1}	Inductor output voltage.
I_p	Primary current
I_L	Inductor current
$I_{L1(pk)}$	Peak Inductor current
$I_{p(avg)}$	Average primary current
$I_{d(max)}$	Maximum drain current
t	Operating mode time
k	Duty cycle
k_{max}	Maximum duty cycle
Ns	Secondary turn number
N_p	Primary turn number
V_{se}	Secondary voltage
T	Period
ΔI	Output current swing difference.
D	Duty rate.
P_o	Output power

P_i	Input power
η	Efficiency
L	Inductor
C	Capacitor
R	Resistance
SOC	State of Charge
PWM	Pulse-Width Modulation
LCD	Liquid-Crystal Display